World Scientific
www.worldscientific.com

MICROENDOSCOPIC SPECTRAL IMAGING AS A TOOL FOR SMALL DUCTUAL DIAGNOSTICS: PRELIMINARY EXPERIENCE

A. DOUPLIK[*,†,‡,§,¶,‡‡], W. L. LEONG[‖], A. M. EASSON[‖],
S. DONE[‡], B. C. WILSON[‡,**], A. SHAHMOON[†] and Z. ZALEVSKY[††]

[*]Department of Physics, Ryerson University
350 Victoria Street, Toronto M5B 2K3, Canada

[†]School of Advanced Optical Technologies (SAOT)
Friedrich-Alexander Erlangen-Nuremberg University, Erlangen, Germany

[‡]Ontario Cancer Institute, University Health Network
Toronto, Canada

[§]Xillix Ltd, Toronto, Canada

[¶]Medical Photonics Engineering Group (MPEG)
Chair of Photonics Technologies
Friedrich-Alexander Erlangen-Nuremberg University, Erlangen, Germany

[‖]Department of Surgical Oncology
Princess Margaret Hospital, University Health Network
Toronto, Canada

[**]Department of Medical Biophysics
University of Toronto, Toronto, Canada

[††]Faculty of Engineering
Bar-Ilan University, Ramat Gan, Israel
[‡‡]douplik@ryerson.ca

A technical feasibility of autofluorescence ductoscopy in breast milk ducts as blood vessels phantoms has been assessed as successful. Malignant tumor can be clearly identified through the milk ducts. We also present the operation principle as well as the preliminary experimental results of a new type of microsize multicore fiber that enables imaging through blood vessel phantoms. Imaging of a manipulated microwire through a drilled phantom is presented.

Keywords: Cancer margin delineation; endoscopy; microendoscopy; autofluorescence imaging; surgical guidance; multicore fibers.

[‡‡]Corresponding author.

1. Introduction

The term "microendoscopy" can be sometimes used for on-site microscopy facilitated by some contemporary endoscopes, but in our particular study this term is employed to describe an endoscope of a very small diameter — usually less than 1 mm. Such a small size allows for the endoscope to penetrate into small hollow ducts including breast ducts. According to the medical statistics in West countries, cancer developed in breast involves a large population, namely incidence rates vary greatly worldwide, with age-standardized rates as high as 1 per 1000 women in North America.[a] Mammary ductoscopy (MD) has been used as a diagnostic tool for ductal carcinoma, which is the most common form of cancer in the breast.[1] The feasibility of the intraductal diagnostics is based on the fact that the malignancies in breasts are frequently developed within the duct epithelium, and hence are detectable via ducts. The ductal carcinoma *in situ* is a non-invasive cancer — the tumor is still located predominantly within the duct, blocking the duct and in breast it may cause so-called nipple discharge, which is considered as an indication for a deep breast examination. The final stage is invasive ductal carcinoma when tumor grows and expands through the ductal wall to the adjacent tissue and start metastasing into surrounding and remote organs. By means of ductoscopy we can conduct patient's surveillance to catch up the early stages of cancer development. Routine palpation, breast ultrasound, mammography, laboratory hormone results, and bacterial culture and cytological results are compulsory during decision-making, mini-endoscopy can be performed for acquiring additional direct visual information from inside the breast duct, which might delay or possibly even prevent potential exploratory operative breast tissue biopsy.[2]

Here, we sought to enhance the diagnostic accuracy of MD by the addition of autofluorescence imaging[1] and diffuse reflectance and fluorescence point spectroscopy.[2] We assessed whether there are distinct changes in the tissue autofluorescence images between malignant and benign tissues that potentially can facilitate visualization of lesions that are not seen under conventional white light ductoscopy.

We also present a new type of a flexible microprobe consisting of multiple core fiber that may facilitate high resolution imaging capabilities as a microendoscope. The main advantages of the suggested microprobe are related to the fact that its external diameter can be relatively small, around $200\,\mu$m, although providing high resolution imaging up to 5000 pixels. Applying a super-resolution technology,[3] the resolution can be further enhanced by at least an order of magnitude.

2. Materials and Methods

For simplicity, we used an existing autofluorescence imaging system that had been developed and optimized for GI endoscopy.[4] *A priori*, this is not necessarily optimal for ductoscopy, so that we included the point fluorescence and reflectance spectroscopies to gain further data that may inform the interpretation of the imaging results and, potentially, to provide additional information that may be used to optimize the imaging parameters for this specific application.

Ten consented patients with a pre-operative diagnosis of palpable invasive ductal carcinoma who required a mastectomy were recruited into the study. This *ex vivo* pilot study was approved by Research Ethics Board at University Health Network, Toronto. All mastectomy specimens were examined within $1-1.5\,$h after resection.

Two different ductoscopes were used. The first three cases were carried out with a 1.1 mm external diameter instrument. However, this was found to limit access, so that the remaining seven cases were done using a 0.7 mm ductoscope. Both devices had a working length of 70 mm, field of view of $70° \pm 5°$ and depth of view of $1-10\,$mm (rigid fiber ductoscope, model MS-611, Fibertech, Japan). The ductoscope was coupled via a standard eyepiece to a fluorescence endoscopic imaging system (OncoLIFE, Xillix Technologies Corp., Canada: now PINPOINT, Novadaq Technologies Corp., Canada).

As shown in Fig. 1, the ductoscope was coupled via a standard eyepiece to a fluorescence endoscopic imaging system (OncoLIFE®, Xillix Technologies Corp., BC, Canada: now PINPOINT®, Novadaq Technologies Corp., ON, Canada). The principle of operation and technical details have been reported elsewhere.[5,6] Briefly, standard white-light and autofluorescence images are recorded at 30 frames per second using 6.3 mW broad-band light and

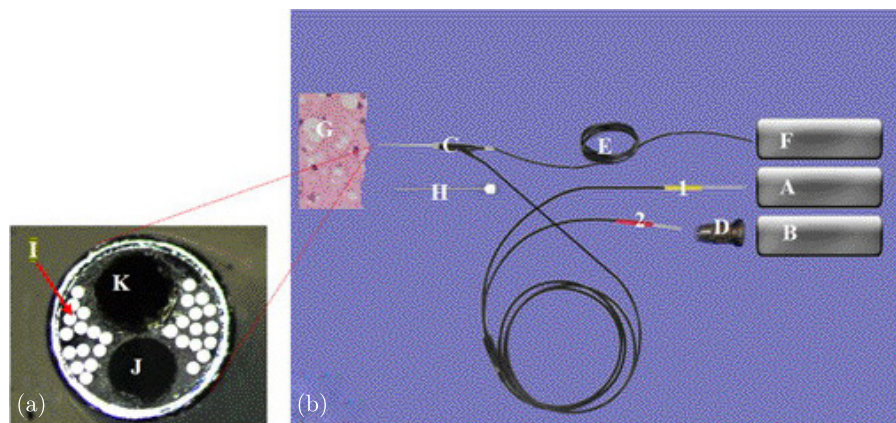---

[a]www.who.int/cancer/detection/breastcancer/en

Fig. 1. Experimental setup for autofluorescence and white-light imaging and for diffuse reflectance and fluorescence point spectroscopies. (a) Close-up of the distal tip of the ductoscope. (b) Schematic of the imaging/spectroscopy elements: (A) endoscopic light source comprising a 200 mW high-pressure mercury arc lamp (VIP R 150/P24 qN2, Osram, Germany); (B) image capture and processing unit, comprising a standard three-color CCD camera for white-light imaging and an intensified CCD camera for autofluorescence imaging; (C) ductoscope (Fibertec, Japan), including the light guide {1} and 3000 fiber imaging bundle {2}; (D) eyepiece for universal mounting; (E) collection fiber for diffuse reflectance spectroscopy (150 μm core silica, NA = 0.22: Thorlabs, USA); (F) combined reflectance and fluorescence spectroscopy unit, including collimating lenses (f/2.7: Edmund Optics, USA), automated filter wheel (AB-300: Spectral Products, USA) and spectrometer (MSL-CS1-USB-VR®: Medspeclab Inc., Canada); (G) tissue (duct wall); (H) biopsy probe; (I) light delivery fibers; (J) imaging guide (with 0.35 mm diameter coupled lenses); and (K) biopsy channel (0.3 mm diameter in the 0.7 mm scope).

5.3 mW blue band (390−450 nm), respectively. The operator can switch between the two modes of imaging rapidly. In fluorescence imaging mode, the endogenous fluorescence (collected within 490−580 nm) is normalized by the red reflectance (690−750 nm) in order to minimize effects due to varying tissue distance and angle or shadowing. In general for other organs, pre-malignant tissues have a reduced green autofluorescence relative to normal tissues when excited by blue light, such that normal tissue appears as cyan, while abnormal tissue is shown as a range of red color in each pixel, depending on the red-to-green ratio. *The point spectroscopy system comprised a small-diameter silica fiber coupled to a fiberoptic spectrometer through an automated filter wheel. The light delivered by the fiberscope was used for illumination/ excitation. The collecting fiber was placed through the biopsy channel and positioned in the center of the imaging field-of-view, gently touching the tissue surface. Two different filters were used: a color-correction filter ("C-filter": Edmund Optics) that balanced the blue and red components of the diffuse reflectance spectrum to be within the detector dynamic range and a customized filter (YF2: Barr Associates, USA) that enabled the green fluorescence to be collected with high efficiency*

(transmission 90% at 455−575 nm) together with a fraction of the diffuse blue and red reflectance (steep cut-off from 90 to 1% transmission between 455 and 445 nm and from 90% to 5% between 575 and 590 nm). The spectra were collected using customized software driving the filter wheel and OncoLIFE® light source to switch at 2.5 Hz between the diffuse reflectance and fluorescence modes and integrating 10−15 spectra in each mode at each observation spot. The integrated fluorescence signal had a standard deviation at a given site of typically ±8% for normal tissue and 15% for cancerous lesions. Based on the reflectance spectra, a total hemoglobin concentration and blood oxygenation was estimated based on Ref. 7.

For the second part of the study, employing the multicore fiber, the images of a microwire inside a channel drilled in a light scattering phantom mimicking human skin were collected for microvessel experiments by means of a flexible multicore fiber. The flexible multicore fiber is considered as a prototype of a next generation flexible microendoscope with higher spatial XY resolution. The experiments were performed using a microprobe prototype with external diameter of 200 μm. Figure 2(a) presents the fabricated phantom. Figure 2(b) shows a 3D view sketch of the phantom
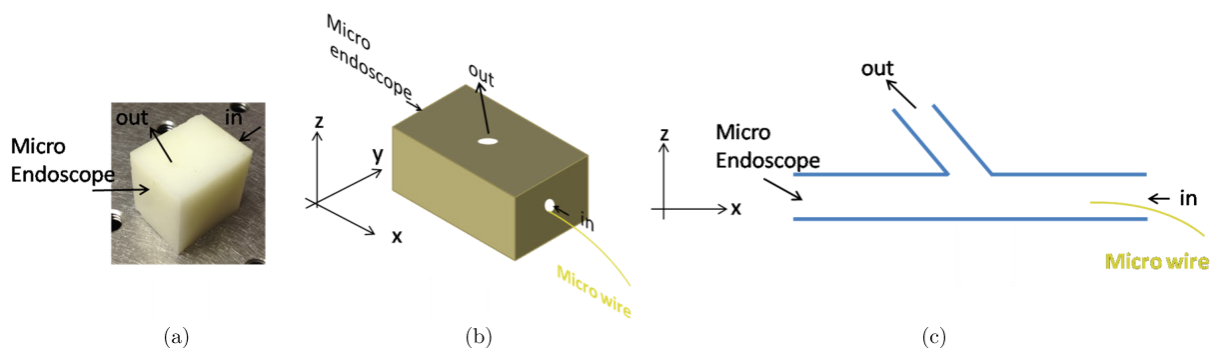
Fig. 2. Phantom configuration. (a) Fabricated phantom. (b) 3D view sketch of the phantom having two drilled channels at diameter of 400 μm. (c) Cross-sectional view of the channels inside the phantom.

having two drilled channels with diameter of 400 μm each. One longitudinal channel (along the x-axis) was drilled from one to the other side of the phantom while another angled channel was made making both channels crossed inside the phantom (Fig. 2(c)). The openings indicated as "in" and "out" formed a flow through system connected with a syringe (Desoi GmbH, Germany) at the entrance ("in"). Figure 2(c) shows a cross-sectional schematic view of the fabricated phantom. Syringe needles (19G) were inserted into the openings in the phantom.

A microwire (stainless steel, 150 micron) imitating a partial blocking of a blood vessel, was inserted onto the "in" opening. A mixture of 1% intralipid (IL) and 5% human hemoglobin (Aldrich Sigma, Germany) and 94% water (imitating human blood) was used as a flow solution flowing through the channels. The other opening ("out") was employed to slide the multicore microprobe inside the phantom to make the microprobe face the microwire.

3. Results and Discussions

Figure 3 shows examples of ductoscopic images, in both white-light and autofluorescence modes, from a 53-year-old woman who underwent a modified radical mastectomy for a 3.5 cm invasive ductal carcinoma (AJCC T2N1M0). As shown in Fig. 3, the images had adequate brightness and resolution in both imaging modes. Figures 3(a) and 3(b) show images taken from a normal duct from the same patient in white-light and fluorescence modes, respectively. In white-light mode, the intraductal carcinoma appeared as irregular protrusions into

the ductal lumen, with color similar to the surrounding ductal tissue (Fig. 3(c)). *The tumor is located in the central area of the image.* In fluorescence mode (Fig. 3(d)), the same intraductal carcinoma appeared reddish compared to the surrounding ductal tissue, which was blue–green (cyan) in color. *It was also observed* that debris seen in the lumen of the normal duct (*result is not shown*), which can be misinterpreted as cancer, appropriately appeared blue–green in fluorescence mode, demonstrating the ability of fluorescence ductoscopy to differentiate cancer from non-cancer tissue in this case.

Figure 4 shows an example of the reflectance and autofluorescence spectra. *It has been found that the blood oxygenation* (SO_2) *in tumor area is* $40\% \pm 25\%$ *lower and total hemoglobin concentration was* $50 \pm 38\%$ *higher. The yellow rectangular margins the current autofluorescence collection setup. It can be anticipated that the contrast can be optimized by approximately* 40% *shifting the cut-off profile of the long-pass interference filter in front of the ICCD camera shifted to the left (green rectangular).*

Figure 5(a) shows the picture of a multicore probe of 15 cm long. Figure 5(b) demonstrates a microscope image of an edge of the probe containing 5000 channels.[8] Each channel is basically a different pixel in the image constructed. Since each channel is rather a single mode than a multimode fiber, the generated image is practically insensitive to bending of the fiber.

Figure 6 presents images of the manipulated microwire obtained by the facing the microprobe inside the channels filled by hemoglobin mixture. Figures 6(a) and 6(b) show different orientation as
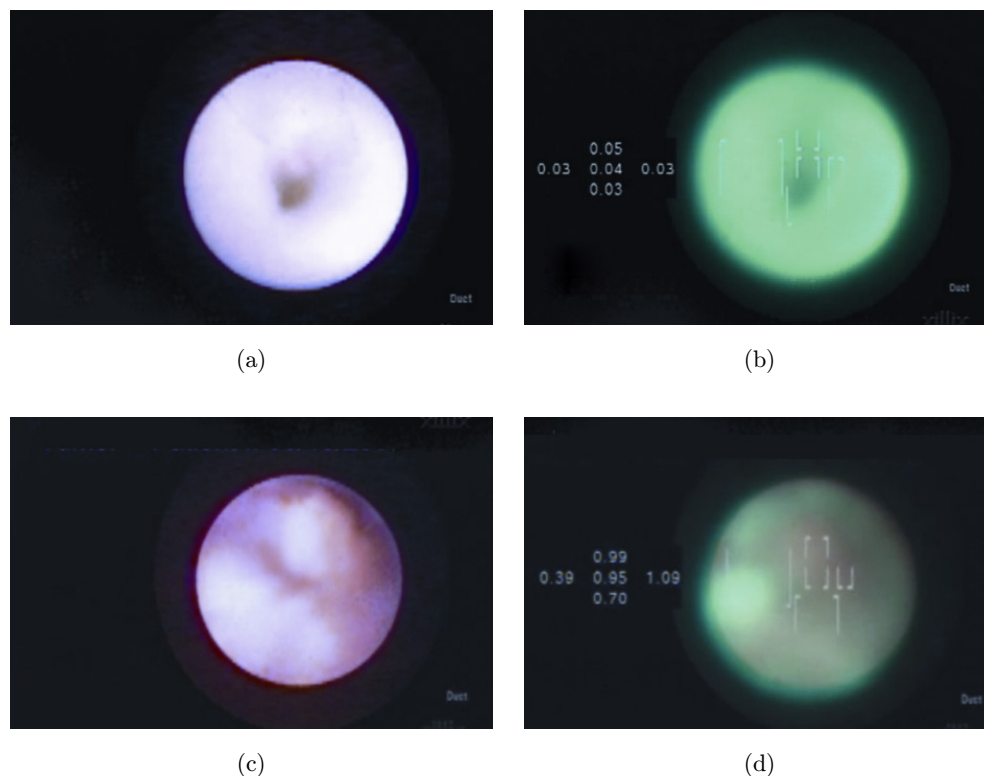
Fig. 3.   Normal region ((a) white light, (b) autofluorescence) compared to tumor region ((c) white light, (d) autofluorescence). *The tumor is located in the central area of the image and can be recognized as reddish patches in the autofluorescence image.* The forward-looking field-of-view view is approximately 1 mm. (Modified from Ref. 4.)
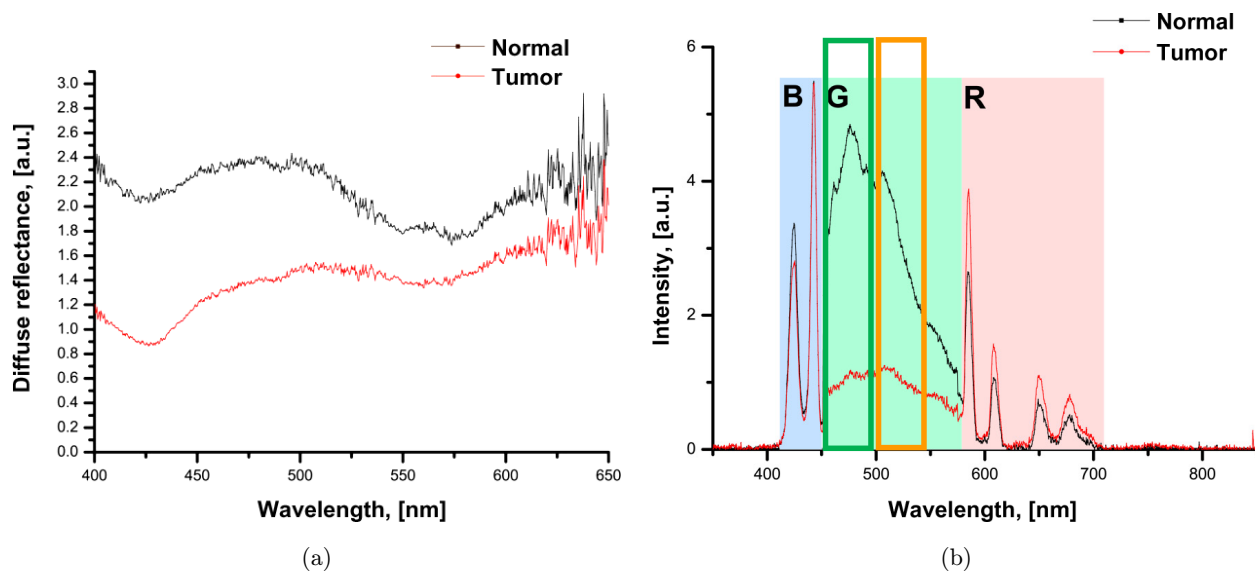

Fig. 4.   (a) Diffuse reflectance spectra over regions of normal and tumor tissue. (b) Autofluorescence spectra in the green band (G) providing also acquisition of some portions of blue (B-band) and red (R-band) reflectance from the excitation light. The sharp peaks within the blue (B) and red (R) bands are mercury lines from the arc lamp source. *The yellow rectangular margins the current autofluorescence collection setup. It can be anticipated that the contrast can be optimized by approximately* 40% *simply shifting the cut-off profile of the long-pass interference filter in front of the ICCD camera (green rectangular).* (Modified from Ref. 4.)
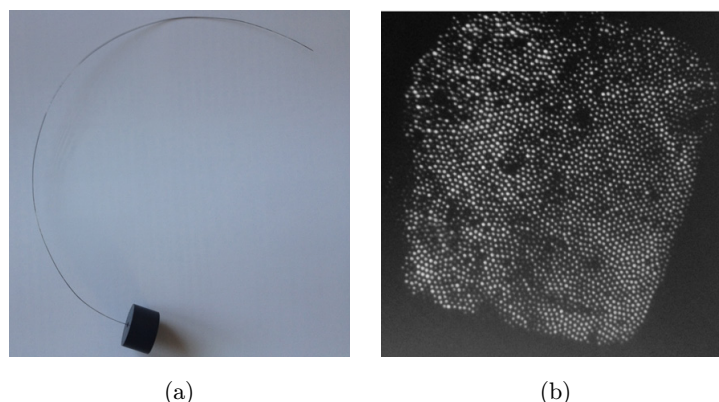
Fig. 5.   (a) A multicore microprobe. (b) Microscope image of the edge of the fabricated microprobe having approximately 5000 optical cores.
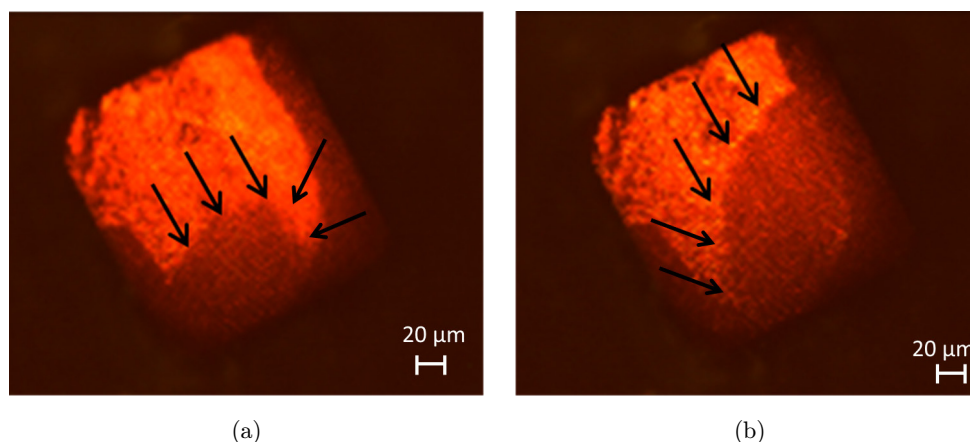

Fig. 6.   Imaging of a manipulated microwire (indicated by the solid arrows) inside an hemoglobin mixture (a) and (b) the imaged microwire at different orientation and positions.

well as positions of the microwire being marked in the figure by several solid arrows. These images validate the circular shape of the microwire.

4.   Conclusions

The point spectroscopy and imaging gave qualitatively similar results. Since ductoscopy can access ducts about $6-10$ cm from the nipple openings, our judgment is that $>95\%$ of breast cancers and papilloma with nipple discharge can be seen.

The next step will be to carry out similar studies *in vivo* and in patients who do not have known malignancy. We also plan to apply hyperspectral imaging system as a versatile tool to discover new algorithms for cancer identification in the future.

In the experimental results we were also able to obtain images of a manipulated microwire

inside hemoglobin mixtures inside channels in the phantom. The phantom is basically mimicking human skin in terms of optical properties such as absorption, scattering coefficients, and phase function of scattering (anisotropy factor). The microwire is imitating a partial block of a blood vessel. The experimental results were carried out using a microprobe prototype having external diameter of $200\,\mu$m providing image resolution of 5000 pixels.

Acknowledgments

References

1. B. Pereira, K. Mokbel, "Mammary ductoscopy: Past, present, and future," *Int. J. Clin. Oncol.* **10**, 112−116 (2005).

2. V. Jacobs, M. Kiechle, B. Plattner, T. Fischer, S. Paepke, "Breast ductoscopy with a 0.55-mm mini-endoscope for direct visualization of intraductal lesions," *J. Minim. Invasive Gynecol.* **12**, 359−364 (2005).

3. V. R. Jacobs, S. Paepke, H. Schaaf, B. C. Weber, M. Kiechle-Bahat, "Autofluorescence ductoscopy: A new imaging technique for intraductal breast endoscopy," *Clin. Breast Cancer* **7**, 619−623 (2007).

4. A. Douplik, W. L. Leong, A. M. Easson, S. Done, G. Netchev, B. C. Wilson, "A feasibility study of auto-fluorescence mammary ductoscopy," *J. Biomed. Opt.* **14**(4), 044036-1-6 (2009).

5. Z. Zalevsky, D. Mendlovic, *Optical Super Resolution* (Springer, 2004).

6. A. Douplik, D. Chen, M. Akens, M. Cirocco, N. Bassett, N. Marcon, J. Fengler, B. Wilson, "Assessment of photobleaching during endoscopic autofluorescence imaging of the lower GI tract," *Lasers Surg. Med.* **42**(3), 224−231 (2010).

7. J. Qu, C. MacAulay, S. Lam, B. Palcic, "Laser-induced fluorescence spectroscopy at endoscopy: Tissue optics, Monte Carlo modeling and in vivo measurements," *Opt. Engrg.* **34**(11), 3334−3343 (1995).

8. A. Shanmoon, H. Slovin, Z. Zalevsky, "Biomedical super resolved imaging using special micro-probe," *BioNano Science Journal* **1**, 103−109 (2011).